Pathological ulna of Amurosaurus riabinini from the Upper Cretaceous of Far Eastern Russia

A pathological ulna of Amurosaurus riabinini from the Upper Cretaceous of Far Eastern Russia

Filippo Bertozzo, Ivan Bolotsky, Yuri L. Bolotsky, Alexey Poberezhskiy, Alastair Ruffell, Pascal Godefroit & Eileen Murphy

INTRODUCTION

Paleopathology is the study of ancient lesions and diseases in the fossil record (Anné et al. 2015), and is an important tool for unveiling new information about immunological responses in extinct species, as well as providing insights concerning their behavior and lifestyle (e.g. Hanna 2002; Farke et al. 2009; Peterson and Vittore 2012; Bell and Coria 2013; Tanke and Rothschild. 2014; Foth et al. 2015; Bertozzo et al. 2017, 2020; Garcia et al. 2017; Xing et al. 2018; Haridy et al. 2019; Bastiaans et al. 2020; Pardo-Pérez et al. 2020). Evidence of disease and injury is detected mainly in the skeletal system, although some soft-tissue injuries can leave a signal in bone (Aureliano et al. 2020). An increasing list of paleopathological lesions is reported for almost every clade of dinosaur, with particularly high frequencies noted in theropods (e.g., Molnar 2001; Bell and Coria 2013; Senter and Juengst 2016) and derived ornithopods (e.g., Rothschild et al. 2003; Tanke & Rothschild 2002, 2014; Siviero et al. 2020; Bertozzo et al. in prep.). These pathologies have been identified as trauma, infection, developmental disorders, tumors, arthritis (Rothschild and Martin 2006; Tanke and Rothschild 2014; Foth et al. 2015), and other conditions, including possible gout (Rothschild et al. 1997; Rothschild and Lambert 2019) and diffuse idiopathic skeletal hyperostosis (DISH - Rothschild and Berman 1991; Bertozzo et al. 2017). Fractures and injuries are the most common and easily identifiable lesions, and they are generally found in areas of the body where they would have been non-life-threatening, such as the caudal vertebrae and digits (Siviero et al. 2020).

Trauma affecting the forelimbs in hadrosaurids are uncommon, and some of those previously identified were serious in nature (Tanke and Rothschild 2014). In a paleopathological survey of an *Edmontosaurus* bonebed undertaken by Siviero et al. (2020), 36 elements from the limbs (excluding the manual bones) were analyzed, but no pathologies were identified. In general, the forelimb region faced a relatively low frequency of injuries and diseases, when compared to areas like the tail or thorax (Bertozzo et al. in prep.). However, several pathological forelimb elements have already been reported. An infection was identified in TMP 1996.017.0009, a hadrosaurid ulna in which the shaft was remodelled and surrounded by an excessive periosteal reaction typical of osteomyelitis, with the mid-shaft appearing to have been previously fractured (FB, pers. obs.). AMNH 5207 is a notably distorted and twisted *Hypacrosaurus* humerus which apparently suffered from an initial transverse fracture, and a subsequent poor healing by misalignment of the separated parts (Tanke and Rothschild 2014). A case of healed fractured zeugopodium is visible in TMP 1996.012.0434, where both the ulna and radius were fractured and later ankylosed as a consequence of callus formation (Tanke and Rothschild 2014). Another well-healed fracture was tentatively identified from a callus formation on the upper half of a hadrosaurid radius (Sawyer and Erickson 1985). Here, the authors suggest that, given the bipedality of these animals, injuries in the front legs were just “minor inconvenience” (Sawyer and Erickson 1985), an assumption challenged by the rarity of such injuries which suggests they had a negative impact on the survival of the affected individuals. Of particular note, Anne et al. (2016) described the first case of septic arthritis in a pathological hadrosaurid ulna from New Jersey. The specimen was characterized by necrosis and reactive bone growth, but no signs of previous trauma were identified. Beyond

Hadrosauridae, a case of severe osteomyelitis (perhaps associated with degenerative osteoarthritis) was identified in the humerus of the ceratopsian *Spiclypeus shipporum*, however this condition appears to have been chronic, lasting several years, thus not directly causing the death of the individual (Mallon et al. 2016). In theropods, several traumas have been found on the forelimbs, including fracture callus in a Late Triassic neotheropod fibula (Griffin 2018); osteomyelitis/septic arthritis on forelimb elements of *Majangasaurus crenatissimus* (Gutherz et al. 2020); fractures in several *Allosaurus* forelimb elements, a tyrannosaurid humerus and an oviraptoroid ulna (Molnar 2001); and a healed fracture on the radius of *Dilophosaurus wetherilli* (Senter and Juengst 2016). Several stress fractures are identified in pedal and manual elements of different sauropod species, such as *Apatosaurus, Barosaurus, Brachiosaurus, Camarasaurus* and *Diplodocus* (Rothschild and Molnar 2005; Tschopp et al. 2014). Bone fractures provide a glimpse into the life of an extinct species, and can reveal new information about intraspecific behavior, prey-predator relationships, locomotion, or unfortunate accidents, such as an impact from an external object.

This paper reports a pathological ulna from the Russian hadrosaurid *Amurosaurus riabinini* (Godefroit et al. 2004), described via morphological and tomographical analyses. The specimen exhibits a marked periosteal reaction at its distal region, suggestive of infectious disease, neoplastic disease, or trauma. The aim of this study is to: i) accurately diagnose the condition responsible for the lesions; ii) suggest a possible cause; and iii) analyze the impact of the pathology on the life of the animal.

MATERIAL AND METHODS

The *Amurosaurus* ulna, AEHM 1/1037, was collected from the Late Cretaceous Udurchukan Formation at Blagoveschensk (Far Eastern Russia). The bone was found in a monospecific bonebed, in association with hundreds of other mostly disarticulated and mixed hadrosaurid remains deposited in a fluvial or alluvial paleoenvironment (Godefroit et al. 2004; Lauters et al. 2008). The specimen was photographed with a Sony Mirrorless a5100 camera, with a focal length of 28 mm at ISO-2500, following standardized directions and a scale bar of 10 cm was added. The total length was measured with callipers, with a minimum error of 1 mm. The pathological area was identified at the distal end of the ulna by comparison with unaffected (= normal) hadrosaurid limb bones and another *Amurosaurus* ulna (AEHM 1/1703). The absence of clear pathognomic features visible externally required examination of the interior of the bone via tomographic scanning, a technique that has already proven useful for enabling diagnosis of such lesions (e.g. Straight et al. 2009; Butler et al. 2013; Anne et al. 2016; Souza Barbosa et al. 2016; Hunt et al. 2019; Ekhtiari et al. 2020). AEHM 1/1037 was scanned at the State Autonomous Healthcare Institution of the Amur Region of Russia with a Philips Brilliance Big Bore CT 16. The specimen was subject to multi-spiral scanning with a slice thickness of 2 mm, under an electronic tube voltage of 120kV at 340 mA, CT dose index (CTDIvol) of 0.16 mGy, following the medical Protocol HEAD for brain scanning. The tomographies were analysed and a 3D model was generated in Radiant Dicom Viewer. The *Amurosaurus* ulna AEHM 1/1703 was also scanned and rendered for comparative purposes following the same procedures. A video of the sagittal view of AEHM 1/1037 is provided in the Supplementary Information, whilst the 3D model can be viewed here: 10.6084/m9.figshare.14986998

RESULTS

Osteological description. AEHM 1/1037 is an isolated right ulna with hadrosaurid affinities (e.g., non-prominent olecranon process, a wide medial process and a thin lateral process distal to the oleocranon). Although it was found disarticulated in a quarry which also yielded material of the hadrosaurine *Kerberosaurus*, the sigmoidal shape of the bone is diagnostic for *Amurosaurus* *riabinini* (Godefroit et al. 2004, 2012b). The specimen is short and sturdy, approximately 32 cm in length when measured from the distal extremity to the proximal end of the olecranon notch. The length is 10.5 times the craniocaudal midshaft width, the same value obtained from the holotype (Godefroit et al. 2004), and shorter than the counterparts of *Edmontosaurus regalis* (14 times; Campione 2014), *Olorotitan arharensis* (11.6 times; Godefroit et al. 2012a), *Hypacrosaurus altispinus* (12 times; Brown 1913), and *Charonosaurus jiayinensis* (12 times; Godefroit et al. 2003). The olecranon notch is missing, probably because of post-mortem taphonomic erosion. The medial process is large and subtriangular, and more developed than the thin lateral process. Between these processes, the articular surface for the proximal portion of the radius is broad and depressed. Towards the midshaft, the ulna maintains a constant width, but the distal end is notably hypertrophied, a marked difference to the narrow and laterally compressed distal end of the holotype and AEHM 1/1703 (see Fig. 1).

Pathological description. The lateral and medial margins of the distal region of the ulna diverge from the main axis, forming a club-shaped end. The surface of this hypertrophic region is strongly irregular, and the occurrence of a jagged and sharp margin in cranial view (corresponding to the fracture site), suggests that pathological bone formation engulfs the distal region of the ulna (Fig. 1D). In caudal view, this pathological overgrowth mostly covers the cranial aspect of the distal region and there are “islands” of indented bone evident on the caudodistal surface (Figs. 1B, 1D). In distal view, the original shape of the articular surface for the carpus is completely lost, although its margins can still be traced (Fig. 1F). Using CT-scanning, the bone shows a well-preserved diaphysis and metaphysis, while the epiphyses is partly preserved. Here, the periosteal and the endosteal regions can be clearly distinguished (Fig. 2B). The distal region is characterized by an irregular circular thickening of the distal metaphysis, corresponding to the callus formation, which engulfs the underlying original portion of the shaft (Fig. 2A, 2C and 3). The thickness of this swollen area is as much as 14.5 mm. On the medial side of the ulna, the cortical layer stops abruptly and is deformed, corresponding to a large bone fracture of the distal end. This fragment is abnormally angled by 16 degrees from the main axis, corresponding to the angulation of the traumatic fracture, and is displaced medially by 8 mm (Fig. 3). The pathological nature of the bone displacement is supported by the tomographic pictures of AEHM 1/1703, in which the bone axis is contiguous, and a consistent width is maintained along the entirety of the length of the bone (Fig. 2D). The distal region of AEHM 1/1703 is regular, and it does not show the extravagant overgrowth of bone surrounding the shaft as in AEHM 1/1037 (Fig. 2D-F). The sigmoidal curvature of the ulna is notably marked in AEHM 1/1037, as a result of the lateral angulation of the fractured distal end. A small subtriangular protuberance in the metaphysis protrudes from the main contour of the fractured fragment within the callus (Fig. 3A).

DISCUSSION

Based solely on the external morphology, possible diagnoses for AEHM 1/1037 include traumatic callus, traumatic infection, and neoplastic growths (aneurysmal bone cyst, osteosarcoma). A callus is a highly vascular fibrous structure containing focal avascular regions of fibrocartilage that envelopes and protects the fractured zone and usually appears some two to three weeks after the injury (Lovell 1997; Rothschild and Martin 2006; Marsell and Einhorn 2011). A fracture callus is formed by woven bone produced by osteoblasts, and hyaline cartilage created by chondroblasts. Once the bone is healed, the callus is subsequently removed and replaced by lamellar bone by osteoblastic/osteoclastic activity (see Marsell and Einhorn 2011 and Nyary and Scammell 2018 for discussions of the healing process). When a fracture does not heal promptly (as in non-union, see Nyary and Scammell 2018), or the fractured bone is exposed to the environment (“open fracture” *sensu* Lovell 1997), it can be at risk of infection by external organisms (bacteria, virus, parasites, or fungi). The intrusion of these external agents can lead to bone responses in the form of periostitis (inflammation of the periosteum) or osteitis (severe infection of the bone and the medullary cavity, such as osteomyelitis) (Lovell 1997). Bone periosteum is elevated from the cortex and responds to the infection-induced inflammation by forming new bone penetrated by the infection, and often developing draining sinuses (Rothschild and Martin 2006). Pathognomic to osteomyelitis is the development of subperiosteal abscesses that lead to necrosis as a consequence of the deprivation of the bone of its blood flow (Lovell 1997). In terms of the potential neoplasms that represent differential diagnoses, an aneurysmal bone cyst is a benign expansile tumor-like bone lesion, mainly located in the metaphysis of long bones, that causes expansion of the cortical margins (Rothschild and Martin 2006), but is usually not associated with pre-existing injuries. Finally, osteosarcoma is a malignant tumor that develops particularly in the metaphysis of human long bones, and is characterized by ill-defined lytic lesions, Codman’s Triangle (elevation of the periosteum away from the cortex) and a spiculated reaction of the periosteum, or “sun-burst” formation (Haun 2006; Rothschild and Martin 2006; Kundu 2014). Based on the displaced distal end along a clear and oblique fractural line, the sub-triangular protrusion along the original outline, and the absence of both cloacae (draining sinuses) and spiculated reactive periosteal bone, it is considered most probable that the lesion is a fracture of the ulnar metaphysis in an advanced state of healing, surrounded by a substantial level of callus. In both human and veterinary medicine, a fracture can be correctly healed by connection and immobilisation of broken bone fragments via plaster and surgical implements, maximising the biology of fracture healing to aid early union and restore function while minimising complications (Nyary and Scammell 2018). With an appropriate treatment, injuries generally start to heal after the third/fourth week, and the process can last for 3-

5 years in humans (Marsell and Einhorn 2011). The time of callus formation and bone healing varies between groups: birds and mammals recover quickly but require a longer period of immobility, while reptiles recover slowly but can move for a short period of time after the injury (Hedrick et al. 2016 and references therein). When artificial immobilisation is absent, the repair processes require a longer time, and are associated with increased risk of fragment displacement and deformation of the limb. In this case, the bone callus surrounds the fractured area due to instability, becoming excessively large. The marked angulation of AEHM 1/1037, of approximately 16 degrees, falls within the range of angular displacement requiring therapy and correction with osteotomy and internal fixation in humans (Rowbotham and Barron 2009). The medial direction of the injured fragment, associated with an excessive level of callus, suggests the bone was undergoing a malunion.

The aggravation of the pathology might have been related to the nature of locomotion of the individual. Debate has long surrounded interpretations of the posture and gait of hadrosaurs. Lull & Wright (1942) represented hadrosaurs in both a bipedal and a quadrupedal posture. During normal progression on land, the total weight of the body was supported by the hindlimbs; the forelimbs were only used for “occasional resting, but neither for progression nor prehension” (Lull & Wright 1942, pg. 87). Ostrom (1964) showed that an aquatic mode of life was unlikely for hadrosaurids and suggested they were terrestrial bipeds; evidences such as the poorly ossified carpus suggests the forelimbs could not have been used to bear weight. Based on limb proportions and the non-graviportal structure of the manus, Galton (1970) proposed that hadrosaurs, and probably all ornithopods, were bipedal and that the vertebral column was probably held more or less horizontal while running. More recently, a general consensus was reached, proposing that in large iguanodontian dinosaurs (including hadrosaurids) a quadrupedal posture could have been maintained for significant periods (e.g. Carrano 2001; Dilkes 2001; Lockley and Wright 2001; Horner et al. 2004; Sellers et al. 2009). Maidment and Barrett (2012) even argued that hadrosaurids possessed all osteological correlates for quadrupedalism. Although its limb proportions cannot be adequately estimated, a series of those osteological correlates can be directly observed in *Amurosaurus*, suggesting that it was as predominantly quadrupedal as other hadrosaurids: it possesses an anterolateral process on the ulna, hoof-like manual unguals, a transversely broadened ilium, and a straight femur with a non-pendant fourth trochanter (Godefroit et al. 2004; Maidment and Barrett 2012). Therefore, the weight-bearing pressure on the wrist would have placed continuous stress on the fracture site, displacing the fractured end of the ulna from the normal axial direction of healing. This most likely would have forced the individual to walk on three limbs, while limping on the fourth (Fig. 4). The fractured ulna, AEHM 1/1037, is much shorter than the healthy ulnae used for comparison purposes (32 cm and 55.5 cm, respectively), and shorter than the holotype ulna (52.5 cm). It can be hypothesized that the relatively shorter ulna of AEHM 1/1037 belonged to a younger individual, but the absence of histological analyses and a growth curve for the species prevents assumptions to be made about the relative maturity of the specimen. Pilon fractures usually result in shortened bones due to the compression of the longitudinal axis (Cruzado-Caballero et al. 2020), but AEHM 1/1037 suffered from an impact fracture, usually characterized by a portion of articular subchondral bone that has broken free of the metaphysis, causing angular deformity and a general widening of the injured site (Wolfe and Katz 1995; Cruzado-Caballero et al. 2020). Thus, the shorter length of the ulna was not a secondary product of the trauma. The fractured area also articulated medially with the distal part of the radius, but the bone hypertrophy is symmetrical between the lateral and medial sides of the ulna so it can be assumed that the articulating radius was also affected. “Foreign” bone pieces engulfed within the callus were not identified in the tomographies, however, and since the radius and carpus were not recovered, it is impossible to know if the injury had involved other adjacent bones.

Identification of the nature of the traumatic event that may have caused an injury is extremely difficult in extinct animal paleopathology, if not impossible. However, some considerations can be made based on the location and direction of the fracture, and the excessive nature of the callus formation and displacement of the fracture parts. Cruzado-Caballero et al. (2020) reports three pathologies in the foot of an *Othnielosaurus*, respectively two fractures (pilon and impact) and calcium pyrophosphate deposition disease (CPPD, an idiopathic condition). Impact fractures can be generated by low forces on the ground, such as running or landing on difficult terrain, whilst pilon fractures are related to a heavy fall on the ground. The latter is usually identified by a vertical compression along the main shaft, resulting from high energy impact on the vertical line, in which the proximal portion of the injured bone penetrates within the distal portion (Cruzado-Caballero et al. 2020). In AEHM 1/1037, the fractured segment is displaced, but it does not push upwards within the proximal portion, and the ulna is not shortened. Instead, the angular orientation, medial to the main axis, and the development of a large fibrous callus are more suggestive of an impact fracture. The animal likely fell/jumped from an upright location, landing on the forelimbs, and fracturing the wrist area. It seems probable that other bones were involved, but this must remain speculative since no other specimens were associated with AEHM 1/1037. The healing process was still active prior to the animal's death, and it seems possible that a correlation between the pathology and death might exist. Despite the possible malunion, no traces of active infection were evident at the fracture site, and it was, therefore, not the direct cause of death (pyogenic infection can spread through the bloodstream in the form of hematogenous osteomyelitis and reach other body regions; McWhinney et al. 2001b). The injury caused the dinosaur to limp, thereby affecting its ability to escape from predators. Hadrosaurids were herd animals (Lockley et al. 1983; Horner et al. 2004; Fiorillo et al. 2014; Hone et al. 2014), and this behavior would have aided the chances of survival of injured individuals who may have stayed hidden within the middle of the herd (Tanke, pers. Comm. 2020). One might suggest the presence of these epimeletic behaviors (Bearzi and Reggente 2018), but they are witnessed only in modern higher mammals, including primates (Campbell et al. 2016), elephants (Sharma et al. 2020) and cetaceans (Warren-Smith and Dunn 2006; Cheng et al. 2018). Epimeletic behaviors in the form of altruism towards young individuals have also been reported for the airborne Common Swifts, *Apus apus* (Tenow et al. 2008), and in the long-tailed skink, *Mabuya longicaudata* (Huang 2006). The presence of such caring behaviors in non-avian dinosaurs, based only on a few fossilized pathologies, is too speculative at this point, and therefore this hypothesis cannot be confirmed at the present time.

CONCLUSIONS

The pathological changes evident on the ulna of *Amurosaurus riabinini*, AEHM 1/1037, are diagnosed as being due to callus that developed after an injury resulting from a fall or stumble on difficult terrain, as suggested by a clear diagonal fracture in the distal section of the shaft. The excessive periosteal reaction, and misalignment of the fractured portion, visible in the tomographies, suggest the fracture was undergoing a malunion and that, if the dinosaur had survived for longer, it would have had a deformed wrist. The animal disrupted the healing process by placing continuous pressure on the pathological areas while walking or standing, resulting in limping and, therefore, a higher chance of being predated. The condition affecting AEHM 1/1037 adds new information about the range of paleopathologies recognized in ornithopod dinosaurs. In particular, forelimb pathologies are under-represented, suggesting that injuries or diseases in these elements were often not compatible with survival. The presence of a healing fracture might also provide circumstantial evidence for a mechanism of "herd defense", in which injured animals gained protection by hiding within large numbers of individuals while on the move. Admittedly, however, inferring such behaviour based on a few pathological specimens cannot be completely accepted. Finally, this study confirms the necessity of analysis of the interior of pathological conditions in fossilized bone so that internal structures can be recognized, and more refined diagnoses obtained.

ACKNOWLEDGEMENTS

We are grateful to A.A. Sorokin and A.P. Sorokin from IGNM FEB RAS that made this study possible. Susannah Maidment (Natural History Museum of London, UK) and Gareth Arnott (Queen's University Belfast) provided thoughtful insights on the study. We thank an anonymous reviewer for the suggestions that improved this manuscript. The research was partly funded by the Queen's University Belfast Culture and Society and Environment Research Clusters. It was undertaken as part of FB's doctoral dissertation within the Horizon 2020 research and innovation programme under the MSCA grant agreement no. 754507 (QUB SPaRK Cohort). All authors confirm there are no conflicts of interest to disclose.

REFERENCES

Anné, J., R. J. Garwood, T. Lowe, P. J. Withers, and P. L. Manning. 2015. Interpreting pathologies in extant and extinct archosaurs using micro-CT. PeerJ 3:e1130.

Anné, J., B. P. Hedrick, and J. P. Schein 2016. First diagnosis of septic arthritis in a dinosaur. Royal Society Open Science 3:160222.

Aureliano, T., C. S. Nascimento, M. A. Fernandes, F. Ricardi-Branco, and A. M. Ghilardi. 2020. Blood parasites and acute osteomyelitis in a non-avian dinosaur (Sauropoda, Titanosauria) from the Upper Cretaceous Adamantina Formation, Bauru Basin, Southeast Brazil. Cretaceous Research 104672.

Bastiaans, D., J. J. Kroll, D. Cornelissen, J. W. Jagt, and A. S. Schulp. 2020. Cranial palaeopathologies in a Late Cretaceous mosasaur from the Netherlands. Cretaceous Research 112:104425.

Bearzi, G., and M. A. Reggente. 2018. Epimeletic behavior. Pp. 337-338 *in* B. Würsig, J. G. M. Thewissen and K. Kovacs, eds. Encyclopedia of marine mammals. Elsevier, Academic Press.

Bell, P. R., and R. A. Coria. 2013. Palaeopathological survey of a population of *Mapusaurus* (Theropoda: Carcharodontosauridae) from the Late Cretaceous Huincul Formation, Argentina. PloS One 8:e63409.

Bertozzo, F., C. Dal Sasso, M. Fabbri, F. Manucci, and S. Maganuco. 2017. Redescription of a remarkably large *Gryposaurus notabilis* (Dinosauria: Hadrosauridae) from Alberta, Canada. Società Italiana di Scienze Naturali e Museo Civico di Storia Naturale, Milano. Volume XLIII:1-56.

Brown, B. 1913. A new trachodont dinosaur, *Hypacrosaurus*, from the Edmonton Cretaceous of Alberta. Bulletin of the American Museum of Natural History 32:395-406

Butler, R. J., A. M. Yates, O. W. Rauhut, and C. Foth. 2013. A pathological tail in a basal sauropodomorph dinosaur from South Africa: evidence of traumatic amputation? Journal of Vertebrate Paleontology 33:224-228.

Campbell, L. A., P. J. Tkaczynski, M. Mouna, M. Qarro, J. Waterman, B. and Majolo. 2016. Behavioral responses to injury and death in wild Barbary macaques (*Macaca sylvanus*). Primates 57:309-315.

Campione, N. E. 2014. Postcranial anatomy of *Edmontosaurus regalis* (Hadrosauridae) from the Horseshoe Canyon Formation, Alberta, Canada. Pp. 208-244 *in* D. A. Eberth and D. C. Evans, eds. Hadrosaurs. Life of the Past, Indiana University Press: Bloomington.

Carrano, M. T. 2001. Implications of limb bone scaling, curvature and eccentricity in mammals and non-avian dinosaurs. Journal of Zoology 254:41-55.

Cheng, Z., M. K. Pine, S. L. Huang, D. Wang, H. Wu, and K. Wang. 2018. A case of epimeletic behavior and associated acoustic records of Indo-Pacific humpback dolphins (*Sousa chinensis*). Journal of Mammalogy 99:1112-1119.

Cruzado-Caballero, P., I. Díaz-Martínez, B. Rothschild, M. Bedell, and X. Pereda-Suberbiola. 2020. A limping dinosaur in the Late Jurassic: Pathologies in the pes of the neornithischian *Othnielosaurus consors* from the Morrison Formation (Upper Jurassic, USA). Historical Biology 1-7.

Dilkes, D. W. 2001. An ontogenetic perspective on locomotion in the Late Cretaceous dinosaur *Maiasaura peeblesorum* (Ornithischia: Hadrosauridae). Canadian Journal of Earth Sciences 38:1205-1227.

Ekhtiari, S., K. Chiba, S. Popovic, R. Crowther, G. Wohl, A. K. O. Wong, D. H. Tanke, D. M. Dufault, O. D. Geen, N. Parasu, M. A. Crowther, and D. C. Evans. 2020. First case of osteosarcoma in a dinosaur: a multimodal diagnosis. The Lancet. Oncology 21:1021-1022.

Farke, A. A., E. D. Wolff, and D. H. Tanke. 2009. Evidence of combat in *Triceratops*. PLoS One 4:e4252.

Fiorillo, A. R., S. T. Hasiotis, and Y. Kobayashi. 2014. Herd structure in Late Cretaceous polar dinosaurs: A remarkable new dinosaur tracksite, Denali National Park, Alaska, USA. Geology 42:719-722.

Foth, C., S. W. Evers, B. Pabst, O. Mateus, A. Flisch, M. Patthey, and O. W. Rauhut. 2015. New insights into the lifestyle of *Allosaurus* (Dinosauria: Theropoda) based on another specimen with multiple pathologies. PeerJ 3:e940.

Galton, P. M. 1970. The posture of hadrosaurian dinosaurs. Journal of Paleontology 44:464–473

García, R. A., I. A. Cerda, M. Heller, B. M. Rothschild, and V. Zurriaguz. 2017. The first evidence of osteomyelitis in a sauropod dinosaur. Lethaia 50:227-236.

Godefroit, P., Y. Bolotsky, and V. Alifanov. 2003. A remarkable hollow-crested hadrosaur from Russia: an Asian origin for lambeosaurines. Comptes Rendus Palevol 2:143-151.

Godefroit, P., Y. L. Bolotsky, and J. Van Itterbeeck. 2004. The lambeosaurine dinosaur *Amurosaurus riabinini*, from the Maastrichtian of Far Eastern Russia. Acta Palaeontologica Polonica 49:585-618.

Godefroit, P., Y. L. Bolotsky, and I. Y. Bolotsky. 2012a. Osteology and relationships of *Olorotitan arharensis*, a hollow-crested hadrosaurid dinosaur from the latest Cretaceous of Far Eastern Russia. Acta Palaeontologica Polonica 57:527-560.

Godefroit, P., Y. L. Bolotsky, and P. Lauters. 2012b. A new saurolophine dinosaur from the latest Cretaceous of Far Eastern Russia. PLoS One 7:e36849.

Griffin, C. T. 2018. Pathological bone tissue in a Late Triassic neotheropod fibula, with implications for the interpretation of medullary bone. New Jersey State Museum Investigations 6:2-10

Gutherz, S. B., J. R. Groenke, J. J. Sertich, S. H. Burch, and P. M. O'Connor. 2020. Paleopathology in a nearly complete skeleton of *Majungasaurus crenatissimus* (Theropoda: Abelisauridae). Cretaceous Research 115:104553.

Hanna, R. R. 2002. Multiple injury and infection in a sub-adult theropod dinosaur *Allosaurus fragilis* with comparisons to allosaur pathology in the Cleveland-Lloyd Dinosaur Quarry Collection. Journal of Vertebrate Paleontology 22:76-90.

Haridy, Y., F. Witzmann, P. Asbach, R. R. Schoch, N. Fröbisch, and B. M. Rothschild. 2019. Triassic cancer—osteosarcoma in a 240-million-year-old stem-turtle. JAMA oncology 5:425-426.

Haun, D. W., N. W. Kettner, and D. K. Bates. 2006. Stress-induced spiculated periosteal reaction appearing as a malignant bone tumor: a case report. Journal of Manipulative and Physiological Therapeutics 29:595-e1.

Hedrick, B. P., C. Gao, A. R. Tumarkin-Deratzian, C. Shen, J. L. Holloway, F. Zhang, K. D. Hankenson, S. Liu, J. Anné, and P. Dodson. 2016. An injured *Psittacosaurus* (Dinosauria: Ceratopsia) from the Yixian Formation (Liaoning, China): implications for *Psittacosaurus* biology. The Anatomical Record 299:897–906.

Hone, D. W., C. Sullivan, Q. Zhao, K. Wang, and X. Xu. 2014. Body size distribution in a death assemblage of a colossal hadrosaurid from the Upper Cretaceous of Zhucheng, Shandong Province, China. Pp. 524-53 *in* D. A. Eberth and D. C. Evans, eds. Hadrosaurs. Life of the Past, Indiana University Press: Bloomington.

Horner, J. R., D. B. Weishampel, and C. A. Forster. 2004. Hadrosauridae. Pp 438-563 *in* D. B. Weishampel, H. Osmólska, and P. Dodson, eds. The Dinosauria, 2nd Edition. University of California Press, Berkeley.

Huang, W. S. 2006. Parental care in the long-tailed skink, *Mabuya longicaudata*, on a tropical Asian island. Animal Behaviour 72:791-795.

Hunt, T. C., J. E. Peterson, J. A. Frederickson, J. E. Cohen, and J. L. Berry. 2019. First documented pathologies in *Tenontosaurus tilletti* with comments on infection in non-avian dinosaurs. Scientific reports 9:1-8.

Kundu, Z. S. 2014. Classification, imaging, biopsy and staging of osteosarcoma. Indian journal of orthopaedics 48:238-246.

Lauters, P., Y. L. Bolotsky, J. Van Itterbeeck, and P. Godefroit. 2008. Taphonomy and age profile of a latest Cretaceous dinosaur bone bed in far eastern Russia. Palaios 23:153-162.

Lockley, M. G., B. H. Young, and K. Carpenter. 1983. Hadrosaur locomotion and herding behavior: evidence from footprints in the Mesaverde Formation, Grand Mesa Coal Field, Colorado. Mountain Geologist 20:5–14.

Lockley, M. G., and J. L. Wright. 2001. Trackways of large ornithopod dinosaurs from the Cretaceous: a review. Pp. 428-442 *in* Tanke, D. H., and Carpenter, K., eds. Mesozoic Vertebrate Life. Indiana University Press, Bloomington and Indianapolis.

Lovell, N. C. 1997. Trauma analysis in paleopathology. American Journal of Physical Anthropology: The Official Publication of the American Association of Physical Anthropologists 104:139-170.

Lull, R. S., and N. E. Wright. 1942. Hadrosaurian dinosaurs of North America. Geological Society of America Special Papers 40**:**1–242.

Mallon, J. C., C. J. Ott, P. L. Larson, E. M. Iuliano, and D. C. Evans. 2016. *Spiclypeus shipporum* gen. et sp. nov., a boldly audacious new chasmosaurine ceratopsid (Dinosauria: Ornithischia) from the Judith River Formation (Upper Cretaceous: Campanian) of Montana, USA. PloS One 11:e0154218.

Maidment, S. C., and P. M. Barrett. 2012. Osteological correlates for quadrupedality in ornithischian dinosaurs. Acta Palaeontologica Polonica 59:53-70.

Marsell, R. and T. A. Einhorn. 2012. The biology of fracture healing. Injury 42:551–555.

McWhinney, L. A., B. M. Rothschild, and K. Carpenter. 2001. Posttraumatic chronic osteomyelitis in *Stegosaurus* dermal spikes. Pp. 141-156 *in* K. Carpenter, ed. The armored dinosaurs. Life of the Past, Indiana University Press: Bloomington.

Molnar, R. E. 2001. Theropod paleopathology: a literature survey. Pp. 337-363 *in* D. H. Tanke and K. Carpenter, eds. Mesozoic Vertebrate Life. Indiana University Press, Bloomington and Indianapolis.

Nyary, T., and B. E. Scammell. 2018. Principles of bone and joint injuries and their healing. Surgery 36:7-14.

Ostrom, J. H. 1964. A reconsideration of the paleoecology of hadrosaurian dinosaurs. American Journal of Science 262:975-997.

Pardo-Pérez, J. M., B. P. Kear, and E. E. Maxwell. 2020. Skeletal pathologies track body plan evolution in ichthyosaurs. Scientific reports 10:1-7.

Peterson, J. E., and C. P. Vittore. 2012. Cranial pathologies in a specimen of *Pachycephalosaurus*. PloS One 7:e36227.

Rothschild, B. M., and D. S. Berman. 1991. Fusion of caudal vertebrae in Late Jurassic sauropods. Journal of Vertebrate Paleontology 11:29-36.

Rothschild, B. M., D. Tanke, and K. Carpenter. 1997. Tyrannosaurs suffered from gout. Nature 387:357-357.

Rothschild, B. M., D. H. Tanke, M. Helbling, and L. D. Martin. 2003. Epidemiologic study of tumors in dinosaurs. Naturwissenschaften 90:495-500.

Rothschild, B. M., and R. E. Molnar. 2005. 17. Sauropod stress fractures as clues to activity. Pp. 381-392 *in* V. Tidwell and K. Carpenter, eds. Thunder-lizards: the sauropodomorph dinosaurs, Indiana University Press: Bloomington.

Rothschild, B. M., and L. D. Martin. 2006. Skeletal impact of disease. New Mexico Museum of Natural History and Science, Bulletin 33.

Rothschild, B. M., and H. W. Lambert. 2019. First documentation of a greenstick fracture in the fossil record. Possible gout also noted in *Arkansaurus fridayii*. Historical Biology 1-3.

Rowbotham, E., and D. Barron. 2009. Radiology of fracture complications. Orthopaedics and Trauma 23:52-60.

Sawyer, G. T., and B. R. Erickson. 1985. Injury and diseases in fossil animals: the intriguing world of paleopathology. Encounters 8:25-28.

Sellers, W. I., P. L. Manning, T. Lyson, K. A. Stevens, and L. Margetts. 2009. Virtual palaeontology: gait reconstruction of extinct vertebrates using high performance computing. Palaeontologia Electronica 12.3.11A.

Senter, P., and S. L. Juengst. 2016. Record-breaking pain: the largest number and variety of forelimb bone maladies in a theropod dinosaur. PLoS One 11:e0149140.

Siviero, B. C., E. Rega, W. K. Hayes, A. M. Cooper, L. R. Brand, and A. V. Chadwick. 2020. Skeletal trauma with implications for intratail mobility in *Edmontosaurus annectens* from a monodominant bonebed, Lance Formation (Maastrichtian), Wyoming USA. Palaios 35:201-214.

Sharma, N., S. S. Pokharel, S. Kohshima, and R. Sukumar. 2020. Behavioural responses of free-ranging Asian elephants (*Elephas maximus*) towards dying and dead conspecifics. Primates 61:129-138.

Straight, W. H., G. L. Davis, H. C. W. Skinner, A. Haims, B. L. McClennan, and D. H. Tanke. 2009. Bone lesions in hadrosaurs: Computed Tomographic Imaging as a guide for paleohistologic and stable-isotopic analysis. Journal of Vertebrate Paleontology 29:315-325.

Souza Barbosa, F. H. de, P. V. L. G. da Costa, L. P. Bergqvist, and B. M. Rothschild. 2016. Multiple neoplasms in a single sauropod dinosaur from the Upper Cretaceous of Brazil. Cretaceous Research 62:13-17.

Tanke, D. H., and B. M. Rothschild. DINOSORES: An annotated bibliography of dinosaur paleopathology and related topics—1838-2001. New Mexico Museum of Natural History and Science Bulletin 20.

Tanke, D. H., and B. M. Rothschild. 2014. Paleopathology in Late Cretaceous hadrosauridae from Alberta, Canada. Pp. 540-571 *in* D. A. Eberth and D. C. Evans, eds. Hadrosaurs. Life of the Past, Indiana University Press: Bloomington.

Tenow, O., T. Fagerström, and L. Wallin. 2008. Epimeletic behaviour in airborne Common Swifts *Apus apus*: do adults support young in flight? Ornis Svecica 18:96-107.

Tschopp, E., O. Wings, T. Frauenfelder, and B. M. Rothschild, B. M. 2014. Pathological phalanges in a camarasaurid sauropod dinosaur and implications on behaviour. Acta Palaeontologica Polonica 61:125-134.

Warren-Smith, Á. B., and W. L. Dunn. 2006. Epimeletic behaviour toward a seriously injured juvenile bottlenose dolphin (*Tursiops* sp.) in Port Phillip, Victoria, Australia. Aquatic Mammals 32:357.

Wolfe, S. W., and L. D. Katz. 1995. Intra–articular impaction fractures of the phalange. The Journal of Hand Surgery 20: 327-333.

Xing, L., B. M. Rothschild, P. S. Randolph-Quinney, Y. Wang, A. H. Parkinson, and H. Ran. 2018. Possible bite-induced abscess and osteomyelitis in *Lufengosaurus* (Dinosauria: sauropodomorph) from the Lower Jurassic of the Yimen Basin, China. Scientific reports 8:1-8.

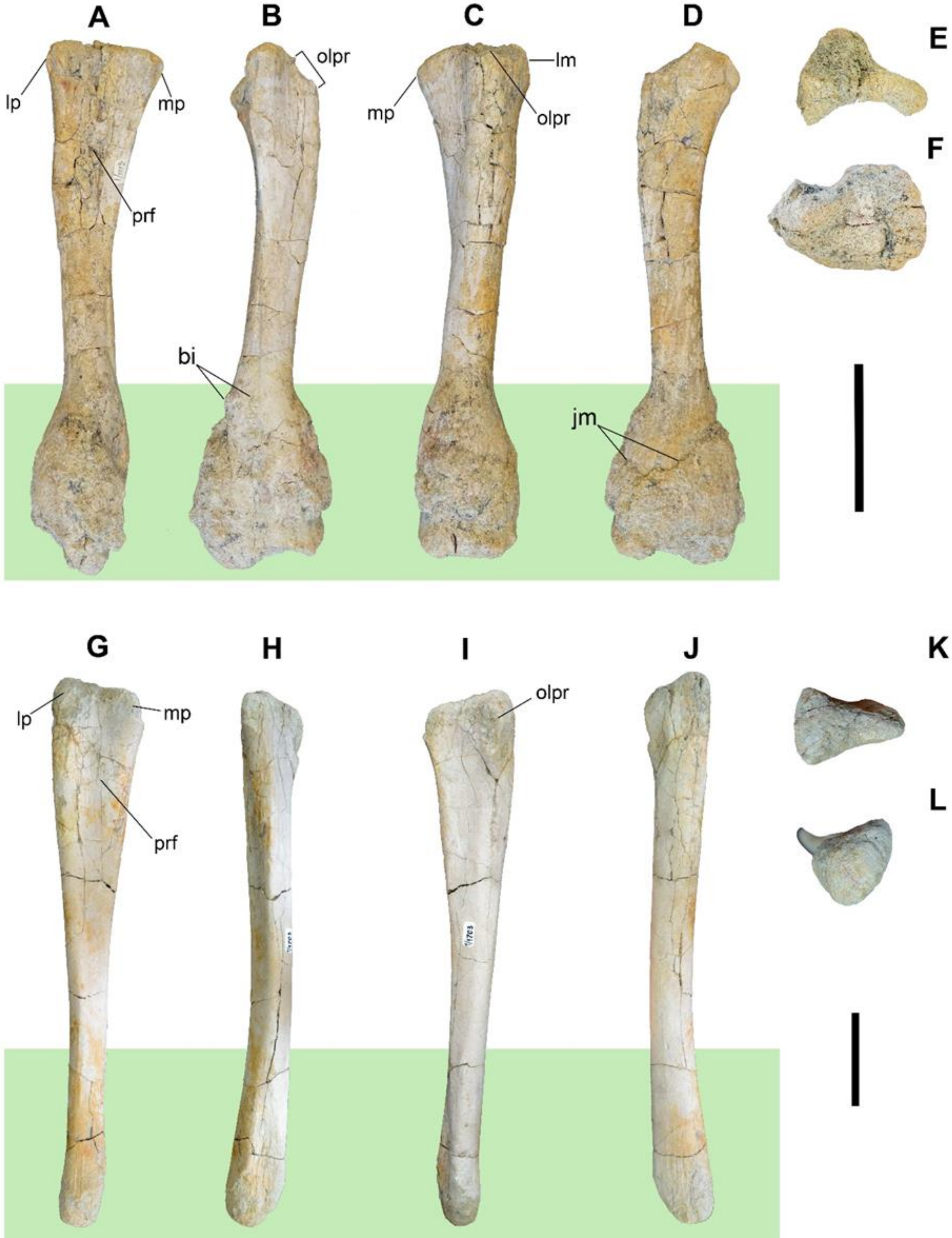

Figure 1 – AEHM 1/1037, the pathological ulna of Amurosaurus riabinini in medial (A), caudal (B), lateral (C), cranial (D), proximal (E) and distal (F) views. AEHM 1/1703, an unaffected

“healthy” ulna of A. riabinini in medial (G), caudal (H), lateral (I), cranial (J), proximal (K) and distal (L) views. The green bars correspond to the distal region, showing the morphological difference attributed to the pathological bone formation. Abbreviations: bi, bone “islands”; lp, lateral process; jm, jagged margin; mp, medial process; olpr, oleocranon process; prf, proximal radial facet. Scale bar = 10 cm.

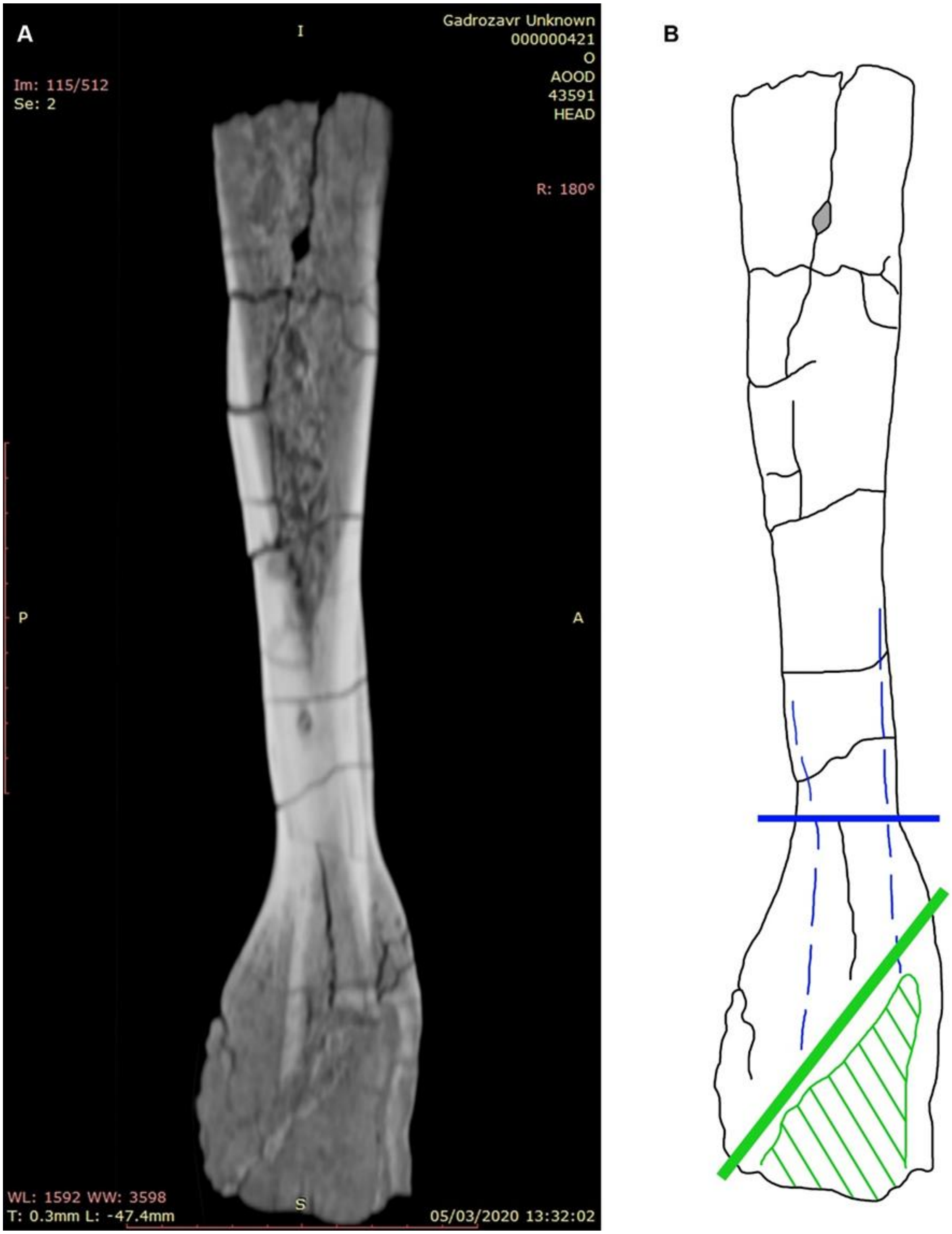

Figure 2 – A) Tomographic picture of AEHM 1/1037, showing the fractured fragment in the distal region of the bone. B) Drawing of the same skeletal element, highlighting the regions of interest. The blue dashed line corresponds to the preserved original ulna shaft engulfed within the callus

formation. The horizontal blue bar defines the beginning of the callus formation. The green oblique lines mark the fractured fragment of the distal portion, while the thick green bar corresponds to the direction of the displacement, resulting in the oblique jagged margin at the fracture site visible in the specimen.

Figure 3 – Artist's impression of a group of *Amurosaurus riabinini* grazing through the ancient forests of Far Eastern Russia, while a Tarbosaurus is pursuing them. The individual in the foreground is limping on the forelimb because of a serious traumatic injury in the right wrist. The injury is swollen, but healing. Artwork by Andrey Atuchin.